



Published in final edited form as:

Cancer Immunol Res. 2020 June ; 8(6): 769–780. doi:10.1158/2326-6066.CIR-19-0483.

Inhibition of MICA and MICB Shedding Elicits NK cell–mediated Immunity against Tumors Resistant to Cytotoxic T cells

Lucas Ferrari de Andrade^{1,2,3,*}, Sushil Kumar^{1,2}, Adrienne Luoma^{1,2}, Yoshinaga Ito^{1,2}, Pedro Henrique Alves da Silva³, Deng Pan^{1,2}, Jason W. Pyrdol^{1,2}, Charles H. Yoon^{4,5}, Kai W. Wucherpfennig^{1,2,6,*}

¹Department of Cancer Immunology and Virology, Dana-Farber Cancer Institute, 450 Brookline Avenue, Boston, MA 02215, USA.

²Department of Immunology, Harvard Medical School, 25 Shattuck Street, Boston, MA 02115, USA.

³Department of Oncological Sciences and Precision Immunology Institute, Icahn School of Medicine at Mount Sinai, 1 Gustave L. Levy Place, New York, NY, 10029-6574, USA.

⁴Department of Medical Oncology, Dana-Farber Cancer Institute, 450 Brookline Avenue, Boston, MA 02215, USA.

⁵Department of Surgery, Brigham and Women's Hospital, 75 Francis Street, Boston, MA 02115, USA.

⁶Department of Neurology, Brigham & Women's Hospital and Harvard Medical School, 25 Shattuck Street, Boston, MA 02115, USA.

Abstract

Resistance to cytotoxic T cells is frequently mediated by loss of MHC class I expression or IFN γ signaling in tumor cells, such as mutations of *B2M* or *JAK1* genes. NK cells could potentially target such resistant tumors, but suitable NK cell–based strategies remain to be developed. We hypothesized that such tumors could be targeted by NK cells if sufficient activating signals were provided. Human tumors frequently express the MICA and MICB ligands of the activating NKG2D receptor, but proteolytic shedding of MICA/B represents an important immune evasion mechanism in many human cancers. We showed that *B2M*- and *JAK1*-deficient metastases were targeted by NK cells following treatment with a monoclonal antibody (mAb) that blocks MICA/B shedding. We also demonstrated that the FDA-approved HDAC inhibitor panobinostat and a MICA/B antibody acted synergistically to enhance MICA/B surface expression on tumor cells. The HDAC inhibitor enhanced MICA/B gene expression, whereas the MICA/B antibody stabilized the synthesized protein on the cell surface. The combination of panobinostat and the MICA/B antibody reduced the number of pulmonary metastases formed by a human melanoma cell line in NSG mice reconstituted with human NK cells. NK cell–mediated immunity induced by

*Corresponding authors: Kai Wucherpfennig, Dana-Farber Cancer Institute, 450 Brookline Avenue, Boston, MA 02215, phone 617-632-3086, Kai_Wucherpfennig@dfci.harvard.edu; Lucas Ferrari de Andrade, Icahn School of Medicine at Mount Sinai, 1425 Madison Avenue, 12-20B, New York, NY 10029, phone 212 659 9585, Lucas.FerrariDeAndrade@mssm.edu.

a mAb specific for MICA/B, therefore, provides an opportunity to target tumors with mutations that render them resistant to cytotoxic T cells.

Keywords

NK cells; MICA; NKG2D; proteolytic shedding; immunotherapy resistance

INTRODUCTION

Checkpoint blockade with antibodies targeting the programmed cell death protein 1 (PD-1) or cytotoxic T lymphocyte-associated protein 4 (CTLA-4) inhibitory receptors on T cells can induce durable antitumor immunity in patients with advanced cancer. However, many patients fail to benefit from these therapies due to primary or secondary resistance (1). Cytotoxic T cells play a central role in the efficacy of checkpoint blockade based on their ability to recognize tumor-derived peptides bound to major histocompatibility complex class I (MHC-I) proteins (2). Recognition of MHC-I-peptide complexes by the T-cell receptor (TCR) triggers T cell-mediated killing via release of cytotoxic granules. Also, secretion of interferon- γ (IFN γ) by T cells inhibits tumor cell proliferation and enhances MHC-I protein expression on both tumor and dendritic cells (3). Resistance to checkpoint blockade is, therefore, frequently mediated by loss of MHC-I expression by tumor cells, either by mutation or epigenetic silencing of key genes in the MHC-I (*B2M*, *TAP1*, *TAP2*, and other genes) or IFN γ (*JAK1*, *JAK2*) pathways (4–6). A low number or loss of neoantigens also diminishes tumor immunity mediated by cytotoxic T cells (7–10). There are no alternative immunotherapies for patients with solid tumors resistant to checkpoint blockade. Chimeric antigen receptor (CAR) T cells could target tumor cells that lack MHC-I proteins, but thus far, CAR T cells have shown limited efficacy against solid tumors (11).

Natural killer (NK) cells recognize tumor cells by molecular mechanisms that differ from those required by cytotoxic T cells. NK-cell recognition of tumor cells is mediated by germline-encoded activating receptors that bind to ligands upregulated on tumor cells by cellular processes associated with malignant transformation, including DNA damage and cellular stress (12). In contrast, T cells recognize MHC-presented peptides derived from shared tumor antigens or neoantigens created by somatic mutations (2). Therefore, tumors resistant to cytotoxic T cells may respond to NK cell-based immunotherapies. In fact, loss of MHC-I expression by tumor cells renders them more sensitive to NK cells because MHC-I proteins serve as ligands for inhibitory NK-cell receptors (12). However, induction of NK cell-mediated tumor immunity may also require effective targeting of immune evasion mechanisms that hinder NK cell-mediated attack. For example, many human cancers express the MHC class I chain-related polypeptide A (MICA) and MICB (MICA/B) proteins that serve as ligands for the activating NK group 2D (NKG2D) receptor on NK cells and subpopulations of T cells (13,14). Tumors frequently evade NKG2D receptor-mediated tumor immunity by proteolytic shedding of MICA/B (15–22). We previously developed monoclonal antibodies (mAbs) that bind to the $\alpha 3$ domain of MICA/B, the site of proteolytic shedding. These mAbs inhibit MICA/B shedding and induce NK cell-mediated tumor immunity. The increased density of MICA/B proteins on tumor cells enhances

NKG2D receptor–mediated activation of NK cells, and the Fc segment of tumor-bound antibodies activates NK cells through the CD16 Fc receptor. Treatment with such MICA/B antibodies induces a shift of tumor-infiltrating NK cells to a cytotoxic state (23).

The *MICA* and *MICB* genes are part of the MHC locus on human chromosome 6, and the encoded proteins share structural similarity with MHC proteins. *B2M* deficiency abrogates T cell–mediated immunity and responsiveness to T-cell checkpoint blockade, but MICA/B proteins do not associate with $\beta 2$ microglobulin or peptides (5,24–26). We hypothesized that inhibition of MICA/B shedding could induce NK cell–mediated immunity against metastatic lesions resistant to cytotoxic T cells. Indeed, treatment with a mAb specific for the MICA/B $\alpha 3$ domain enabled NK cell–mediated immunity against tumors with inactivating mutations in the MHC-I or IFN γ signaling pathways (*B2m* and *Jak1* mutations, respectively). Also, it is known that the *MICA/B* genes are epigenetically regulated by histone deacetylases, which inhibit MICA/B expression by tumor cells (27–30). We found that a HDAC inhibitor acted synergistically with a MICA/B mAb *in vivo* to enhance MICA/B protein expression on the surface of tumor cells through enhanced transcription of *MICA/B* genes (via the HDAC inhibitor) and inhibition of MICA/B shedding (via the MICA/B mAb). This combination therapy conferred NK cell–mediated immunity against melanoma metastases in a humanized mouse model.

MATERIALS AND METHODS

Cell lines

B16F10, LLC1, A375, HCT-116, A549, and U937 cell lines were purchased from ATCC (Manassas, Virginia). RPMI-8226 and U266 cell lines were generously donated by Dr. Irene Ghobrial (Dana-Farber Cancer Institute, Boston, Massachusetts), and the NCI-H139-Sqc cell line was generously donated by Bristol-Myers Squibb (Redwood City, California). The CY029-S1, CY048-S, CY 21A-S1, CY.119–1A S, and CY36-S1 short-term melanoma cell lines were previously described (23,31). All cell lines tested negative for mycoplasma prior to use in experiments using the Universal Mycoplasma Detection Kit (ATCC, catalog number 30–1012K) or MycoAlert™ Mycoplasma Detection Kit (Lonza, catalog number LT07–318). All cell lines were used within a small number of passages (approximately less than 10 passages) after they had been obtained from vendors or collaborators between the years of 2015 and 2019. A375, HCT-116, A549, U937, RPMI-8226, U266, and NCI-H139-Sqc cell lines were cultured in RPMI-1640 media, whereas the B16F10, LLC1, CY029-S1, CY048-S, CY 21A-S1, CY.119–1A S, and CY36-S1 were grown in DMEM media. RPMI-1640 and DMEM media were supplemented with 10% FBS, 1x Glutamax, and 1x penicillin/streptomycin. All tissue culture reagents were purchased from Gibco (Thermo Fisher Scientific). Cells were cultured at 37 °C with 5% CO₂.

Control and *B2M*-KO A375 cells were generated by transducing parental A375 cells with a lentiCas9-blast vector (Addgene #52962) followed by selection with blasticidin (Gibco, catalog number R21001). Subsequently, cells were transduced with pLKO3G-gRNA-PGK-EGFP vector, which was reported previously (32), with a gRNA targeting the human *B2M* genes inserted between the BsmB1 sites. The control cell line was transduced with the backbone of the vector. Following transduction, cells were cultured for 24 hours in the

presence of recombinant human IFN γ (10 ng/mL, BD Biosciences) to induce upregulation of MHC-I proteins. Cells were stained with APC-conjugated W6/32 antibody (clone W6/32, Biolegend, catalog number 311410), and HLA-A/B/C-negative *B2M*-KO cells and HLA-A/B/C-positive control cells were sorted by flow cytometry (BD FACS Aria III). As shown in Figure 1A and Supplementary Figure S1A–B, 100 % of the isolated cell population was *B2M*-KO. Parental A375 cells were also transduced with a pHAGE lentiviral vector (Harvard Gene Therapy Center) to enable expression of ZsGreen under the control of the EF1 α promoter. This vector was generated by inserting the ZsGreen sequence between the NotI and BamHI restriction sites, which removed an IRES and ZsGreen sequence from a parental vector. ZsGreen⁺ A375 cells were sorted by flow cytometry (BD FACS Aria III) and used to examine MICA/B expression *in vivo*.

The B16F10 control and *B2m*-KO cell lines were previously reported (32). MICA expression was achieved by transduction of control and *B2m*-KO B16F10 cells with a pHAGE lentiviral vector that carried a MICA*009-IRES-luciferase expression cassette under the control of the EF1 α promoter. This plasmid was reported previously (23). The B16F10 control and *B2m*-KO cell lines were labelled with PE-conjugated anti-MICA/B (Biolegend catalog number 320906), and MICA⁺ cells were sorted by flow cytometry (BD FACS Aria III). *Jak1*-KO B16F10-MICA cells were generated by electroporation of the control B16F10-MICA cell line with Cas9 protein and a gRNA targeting the *Jak1* gene (sequences in Supplementary Table S1). Electroporation was performed using the Amaxa™ SF Cell Line 96-well Nucleofactor™ Kit (Lonza, V4SC-2096) in a 4D Nucleofactor (Lonza). Cells were treated for 24 hours with IFN γ (10 ng/mL, BD Biosciences). Subsequently, cells were labeled with PE-conjugated MICA 6D4 antibody (Biolegend, catalog number 320906) and a cocktail of APC-conjugated MHC-I antibodies (anti-H-2K^b and anti-H-2D^b, Biolegend catalog numbers 116518 and 111513, respectively). MICA⁺MHC-I⁻ *B2M*-KO and MICA⁺MHC-I⁺ control B16F10 were then sorted by flow cytometry (BD FACS Aria III).

LLC1 cells were first transduced with a pHAGE lentiviral vector that carried a MICA*009 cDNA – IRES – ZsGreen expression cassette under the control of an EF1 α promoter (Addgene #114007). The resulting LLC1-MICA cells were electroporated with Cas9 protein and bound gRNAs targeting the *B2m* gene. Control cells were electroporated with Cas9 protein alone. Control and *B2m*-KO LLC1-MICA cells were treated with IFN γ (10 ng/mL; BD Biosciences) for 24 hours and sorted by flow cytometry based on expression of H-2K^b (clone AF6–88.5 Biolegend). Control LLC1-MICA cells were H-2K^b-positive, whereas *B2m*-KO LLC1 cells were H-2K^b-negative.

Western blotting

B16F10, LLC1, and A375 cell lines were treated with or without IFN γ (50 ng/mL; BD Biosciences) for 16 hours in DMEM supplemented with 10 % FBS (Life Technologies). Subsequently, cells were washed in PBS and lysed in RIPA Lysis and Extraction Buffer (Thermo Scientific, 89901) supplemented with a protease inhibitor cocktail (Sigma Aldrich, P8340). Lysates were centrifuged for 10 minutes at 14,000 rpm, 4 °C. Total protein was measured by Pierce BCA Protein Assay Kit (Thermo Scientific, 23225) and normalized

prior to gel loading to 20 µg total protein per lane. Following SDS-PAGE, samples were transferred to polyvinylidene difluoride membrane (Bio-Rad Sequi-Blot PVDF, 1620184), which was blocked in 5 % milk in Tris-buffered saline supplemented with 0.1% Tween. Blots were then incubated overnight with the appropriate primary antibodies: (1:2000 dilution): rat anti-mouse B2M (R&D Systems, mab8325), rabbit anti-human B2M, JAK1, GAPDH, and tubulin (Cell Signaling Technology, 12851, 3344, 8884, 2144). Following 1 hour incubation with HRP-conjugated anti-rat (Cell Signaling Technology, 6502; 1:3000) or anti-rabbit (Jackson ImmunoResearch, 211-032-171; 1:10,000) secondary antibodies, proteins were visualized by chemiluminescence (Western Lightning and Perkin-Elmer, NEL104001EA) using a Chemi-Doc MP Imaging System (Bio-Rad Laboratories).

MICA/B shedding assays

5×10^4 tumor cells (A375, Control A375, B2M-KO A375, CY048-S, CY029-S1, CY.119-1A-S, CY36-S1, CY 21A-S1, HCT-116, A549, RPMI-8226, U266, U937, NCI-H139-Sqc) were cultured for 24 hours in 96-wells plates (flat-bottom for adherent cells or U-bottom for suspension cells) in the presence of different concentrations of antibodies (7C6 or isotypes control clones C1184, MPC-11, or BE0086; all isotypes were from BioXcell), IFN γ (ranging from 10 to 0.01 ng/mL), and/or panobinostat (ranging from 1000 to 0.01 nM, ApexBio, catalog number A8178), as indicated in each figure. Following a 24-hour culture period, plates were centrifuged for 5 minutes at $500 \times g$, and supernatants were collected for analysis of shed MICA using the Human MICA ELISA Kit (Abcam, catalog number ab59569). To do so, supernatants were diluted 1:2 in the standard dilution buffer provided by the kit, and concentrations were calculated with a standard curve utilizing recombinant MICA variant 008 (ranging from 2000 to 31.25 pg/mL). Plates were read in an EnVision $^{\circledR}$ microplate reader (Perkin Elmer). MICA concentrations were calculated using GraphPad Prism 8 software. We previously demonstrated that the 7C6 mAb does not interfere with detection of MICA shedding using this ELISA (23).

Adherent cells were detached with Versene (Gibco, catalog number 15040-066) to preserve the integrity of MICA/B proteins on the cell surface. Fc receptors were blocked using Human TruStain FcX $^{\text{TM}}$ (Biolegend, catalog number 422302), and cells were stained with PE or APC-conjugated anti-human MICA/B clone 6D4 (Biolegend, catalog numbers 320906 or 320908, respectively). The 6D4 antibody binds to the α 1- α 2 domains of MICA/B and thereby does not compete with the 7C6 antibody that targets the α 3 domain of MICA/B, as shown previously (23). Cells were also stained with dead cell markers, either 7-AAD (BD Pharmingen $^{\text{TM}}$, catalog number 559925), Zombie UV, Yellow, or Near Infrared (Biolegend, catalog numbers 423108, 423104, and 423106, respectively). Data were acquired using a BD Fortessa X20 or Beckman Coulter CytoFLEX LX, and analyses were performed using FlowJo V10 software.

Mice

Wild-type (WT) C57BL6/J, OT-1, *Ighm* $^{-/-}$ C57BL6/J, CB6F1/J, and NSG mice were purchased from the Jackson Laboratories (catalog numbers 000664, 003831, 002288, 100007, and 005557, respectively). *Rag2* $^{-/-}$ *Il2rg* $^{-/-}$ knockout mice were purchased from Taconic (catalog number 4111). Mice were male (except for NSG mice that were female)

and 6–8 weeks of age. Mice were housed in the vivarium of the Dana-Farber Cancer Institute and Icahn School of Medicine at Mount Sinai. The institutional committees for animal use approved the procedures used in this study.

Isolation of human and murine NK cells

Human NK cells from healthy individuals (leukoreduction collars) were isolated by negative selection using the EasySep™ Human NK-cell Isolation Kit (Stem Cell Technologies, catalog number 17955), which resulted in NK-cell purities of at least 90%. Leukoreduction collars were provided in an anonymous manner by Brigham and Women's Hospital (Boston, USA). A total of three leukoreduction collars were used in this study. NK cells were expanded *in vitro* in G-Rex 6-wells plates (Wilson Wolf, catalog number 80240M) using RPMI-1640 media supplemented with 10% FBS, 5% human AB serum (Valley Biochemical), IL2 (1,000 U/mL), and IL15 (20 ng/mL)(both cytokines were from BD Biosciences). Media was replenished once per week until NK cells were used for experiments between 1–3 weeks since isolation.

Murine NK cells from tumor-free C57BL/6 mice or CB6F1 were isolated by meshing spleens using a 70 µm cell strainer, followed by red cell lysis (ACK buffer, Gibco) and staining with PE-conjugated anti-mouse CD49b (Biolegend, catalog number 108908) and APC-conjugated anti-mouse CD3e (Biolegend, catalog number 100312). NK cells were sorted by flow cytometry (BD FACS Aria III), yielding typical purities of ~99%. (2×10^5 cells) were immediately injected via tail vein in *Rag2^{-/-}Il2rg^{-/-}* KO mice for experiments involving allogeneic or syngeneic NK cells.

NK cell-mediated killing assays

For long-term NK cell-mediated killing assays, 1×10^6 GFP⁺ control and *B2M*-KO A375 cells were pretreated for 24 hours with MICA/B or isotype control mAbs (20 µg/mL) in RPMI-1640 media supplemented with 10% FBS, 1x Glutamax, and 1x penicillin/streptomycin. Subsequently, tumor cells were detached with Versene, washed with PBS, and plated in black-wall 96-well plates (Corning™, catalog number 3603) at a density of 5×10^3 cells per well. Human NK cells were added 1–2 hours later at different effector to target ratios as indicated in the figures, and IL2 (300 U/mL, BD Biosciences) was added to support NK-cell survival. The number of GFP⁺ tumor cells was tracked over time for a total of 72 hours using a Celigo Image Cytometer (Nexcelom Bioscience, Lawrence, USA), as reported previously (33).

For short-term NK-cell killing assays, 1×10^6 A375 melanoma cells were pretreated for 24 hours with MICA/B or isotype control mAbs (20 µg/mL) in tissue culture media and then used as target cells in 4-hour ⁵¹Cr-release assays, as described previously (23). Healthy donor-derived human NK cells were isolated by negative selection from leukapheresis reduction collars, as described above, and cultured for 24 hours with IL2 (1,000 U/mL; BD Biosciences) in 96-wells U-bottom plates prior to use in the assay. In some experiments, KIR receptors on NK cells were blocked in the ⁵¹Cr-release assay by addition of an isotype control mAb (10 µg/mL) or anti-KIR2DL2/3 plus anti-KIR2DL4 (BioLegend, catalog numbers 312602 and 347003).

CD8⁺ T-cell cytotoxicity assay

To confirm resistance of *Jak1*-KO and *B2m*-KO B16F10-MICA cell lines to CD8⁺ T cell-mediated cytotoxicity, a Celigo-based image cytometry assay was performed (33). Briefly, 2×10^6 tumor cells were pulsed with 10 nM OVA (SIINFEKL) peptide (Sigma, catalog number S7951) overnight, washed with PBS, and added to 96-well plates (5,000 tumor cells per well). Naïve OT-I CD8⁺ T cells were isolated from the spleens of OT-I mice (JAX stock number 003831) using EasySep™ Mouse CD8⁺ T-cell Isolation Kit (StemCell Technologies Inc., catalog number 19853) according to manufacturer's protocol. The tumor cells were cocultured with naïve OT-I CD8⁺ T cells at different effector to target ratios (1:0 no T cells; 1:1, 2:1, and 5:1; 8–10 replicates per group). 48 hours later, supernatants were removed, and wells were washed with PBS to remove dead tumor cells and CD8⁺ T cells. The plate was then analyzed using the Celigo instrument for quantification of live tumor cells.

Bulk RNA-seq analysis of human A375 melanoma cells

Parental A375 cells (1×10^6 cells) were treated for 24 hours with panobinostat (50 nM) or the corresponding volume of PBS. Cells were then detached with Versene, and RNA was isolated with RNeasy Plus Mini Kit and RNase-Free DNase Set, respectively (both Qiagen kits, catalog numbers 74134 and 79254, respectively). Generation of cDNA, sequencing, and analyses were done as previously reported (23). Briefly, RNA sequencing libraries were generated using the Kapa mRNAseq kit (KapaBiosystems), analyzed by Next-Generation Sequencing, and pooled barcoded samples were subjected to VIPER analysis. Data were also analyzed by Gene Set Enrichment Analysis 4 (Broad Institute) software. Data were deposited in the Gene Expression Omnibus (accession number GSE145447).

Real-time quantitative PCR (qPCR)

A375 cells (1×10^6 cells) were treated for 24 hours with panobinostat (50 nM). Subsequently, cells were washed twice with PBS, pelleted, and used for extraction of total RNA using the RNeasy mini kit (#74106, Qiagen) according to the manufacturer's protocol. One microgram of the extracted RNA was used to synthesize cDNA using SuperScript IV VILO Master Mix (ThermoFisher, 11756050). Diluted cDNA was used for qPCR using TaqMan Gene Expression MasterMix (Life Technologies, 4369016), TaqMan probes (MICA - Hs00741286_m1, MICB - Hs00792952_m1, GAPDH - Hs02786624_g1, ULBP2 - Hs00607609_mH, and RAET1L - Hs04194671_s1) and QuantStudio 6 Flex Real-Time PCR System (ThermoFisher). To examine changes in gene expression between groups, CT values were determined from mean CT values of three technical replicates per sample in each group. Fold change in gene expression was represented relative to *GAPDH* (a housekeeping gene) for each sample.

Metastasis models in immunocompetent mice

B16F10-MICA tumor cells (control, *B2m*-KO or *Jak1*-KO) were inoculated intravenously into C57BL/6 mice (WT or *Ighm*^{-/-}) via the tail vein (1.0 to 7×10^5 cells in 100 μ L of PBS depending on the experiment, as described in figure legends). Treatment was initiated in *Ighm*^{-/-} mice when mice had established metastases (day 7 following tumor inoculation) by intraperitoneal injection of isotype control mAb (BioXcell, catalog number BE0085) or

7C6-mIgG2a mAb (200 µg per injection, days 7, 8, and then once per week). In an alternative protocol, WT mice (*Ighm*^{+/+}) received antibody injections on days 1, 2, and then once per week. Antibodies that induced depletion of CD8⁺ T cells (100 µg anti-CD8β, BioXcell, catalog BE0223) or NK cells (1:10 dilution anti-asialo GM1, Wako Chemicals, catalog 986-10001, and 100 µg anti-NK1.1, clone PK136, BioXcell) were injected via intraperitoneal route on days -1, 0, and then once per week relative to tumor cell inoculation. Murine IgG1 was used as control IgG (BioXcell, catalog BE0083). Lungs were harvested and metastases were quantified on day 14 under a stereomicroscope following formalin fixation of the tissue. Alternatively, the survival of mice was recorded.

For the LLC1-MICA metastasis model, WT C57BL/6 mice were inoculated intravenously via the tail vein with 1.0 to 1.5×10⁶ tumor cells (as indicated in the figure legends) in 0.1 mL of PBS. 7C6-mIgG2a or isotype control mAbs (200 µg) were administered on days 2, 3, and then once per week relative to tumor cell inoculation. For experiments involving adoptive transfer of NK cells, 2×10⁵ NK cells isolated from the spleens of WT C57BL/6 (syngeneic) or CB6F1/J (allogeneic) mice were injected intravenously into *Rag2*^{-/-}*Il2rg*^{-/-} knockout mice. These NK cells were isolated by flow cytometry as CD3e⁻CD49b⁺ cells. LLC1-MICA tumor cells (7×10⁵ cells) were injected intravenously one day following NK-cell transfer. 7C6-mIgG2a or isotype control mAbs (200 µg/injection) were given intraperitoneally on days 2, 3, and then once per week. On day 14, mice (WT or *Rag2*^{-/-}*Il2rg*^{-/-} knockout) were euthanized by CO₂ inhalation, and Indian ink (30%) was injected into the trachea to enable counting of lung metastases, as previously described (34). Lung tissue was treated using Fekete's fixative and surface metastases were counted using a stereomicroscope.

Characterization of murine NK cells in the B16F10-MICA metastasis model

WT C57BL/6 mice were inoculated intravenously with 7×10⁵ B16F10-MICA cells that either had the control, *B2m*-KO, or *Jak1*-KO genotype. Mice were treated with 7C6-mIgG2a or isotype control mAbs (200 µg/injection) on days 1 and 3 following tumor cell inoculation. On day 12, mice were injected intravenously with 50 µL of APC-conjugated anti-mouse CD45.2 (Biolegend, 109814) to label intravascular immune cells and then were euthanized. Harvest lung tissue was cut into small pieces, resuspended in RPMI-1640 supplemented with collagenase type IV (1 mg/mL, Gibco), hyaluronidase (0.1 mg/mL, Sigma), and DNase (20 U/mL, Sigma) and processed using a gentleMACS Octo Dissociator with Heaters (Miltenyi) using C tubes (Miltenyi) with the program 37C_m_LDK_1. The cell suspension was then filtered at 70 µm and incubated with mouse TruStain FcX™ (Biolegend, catalog number 101320) and multiple antibodies: PE-Cy7-conjugated anti-mouse CD45.2 (Biolegend, 109830), APC-conjugated anti-mouse CD3e (Biolegend, 100312), APC-conjugated anti-mouse TCRβ (Biolegend, 109212), BV785-conjugated anti-mouse NK1.1 (BD Biosciences, 740853), PE-CF594-conjugated anti-mouse CD49b (BD Biosciences, 562453), Alexa488-conjugated anti-mouse EOMES (Invitrogen, 53-4875-82), PE-conjugated anti-mouse GZMA (Invitrogen, 12-5831-82), BV421-conjugated anti-mouse NKG2D (BD Biosciences, 562800), PERCP-CY5.5-conjugated anti-mouse CD16/32 (Biolegend, 101324), BV510-conjugated anti-mouse Ly49C/I (BD Biosciences, 744028), and Zombie UV (Biolegend, 423108). Cells were analyzed using a CytoFLEX Flow Cytometer (Beckman Coulter), and data were processed using FlowJo V10.

Humanized mouse model

NSG mice were inoculated intravenously with human NK cells (1 to 2×10^6 cells) that had been expanded *in vitro* as described above. IL2 (Peprotech, catalog number 200–02) was injected intraperitoneally (7.5×10^4 units) to support *in vivo* survival of NK cells, as previously reported (23). A375 melanoma cells (5×10^5 cells, control or *B2M*-KO) were injected one day later (day 0). One day after tumor cell inoculation, mice received another dose of IL2 (75,000 U) plus isotype control (BioXcell, catalog BE0096) or 7C6-hIgG1 mAbs (200 μ g), as well as PBS or panobinostat (10 mg/kg; ApexBio, catalog number A8178). On day 2, mice were again reconstituted with human NK cells from the same donor and also received injections of IL2, antibodies, as well as PBS or panobinostat. Metastases in the lungs were quantified two weeks after the last treatment, as described above for the LLC1-MICA metastasis model (injection of Indian ink into the trachea, treatment of lung tissue with Fekete's fixative).

NSG mice were inoculated with 1×10^6 ZsGreen⁺ A375 melanoma cells to study the effect of MICA/B mAb and panobinostat treatment on MICA/B surface expression in lung metastases. These mice did not receive human NK cells. When metastases were established (two weeks later), mice were treated on two subsequent days with 7C6-hIgG1 or isotype control mAbs (200 μ g), as well as panobinostat (10 mg/kg) or PBS as a solvent control. One day following the last treatment, mice were euthanized by CO₂ inhalation, and lung tissue was dissociated mechanically as explained above but without the use of enzymes to preserve the integrity of MICA/B proteins. Tumor cells were identified as viable large cells that were ZsGreen⁺ but negative for the murine CD45 antigen. MICA/B surface protein was labeled with a 6D4-PE mAb (Biologend, catalog 320906) and quantified by flow cytometry (Beckman Coulter CytoFLEX LX) and analyzed by FlowJo v10.

Characterization of human NK cells in tumor-free NSG mice

Tumor-free NSG mice were inoculated intravenously with 2×10^6 human NK cells that were expanded *in vitro* as described above. At the same time, mice also received intraperitoneal injections of IL2 (7.5×10^4 , Peprotech), as well as panobinostat (10 mg/kg) or PBS as the solvent control. One day later, blood was collected via retro-orbital bleeding, and human NK cells were analyzed by flow cytometry as described.

Statistical analyses

All statistical analyses were performed using GraphPad Prism 8 software, and the relevant statistical tests are indicated in each figure legend.

RESULTS

NK cell–mediated killing of human *B2M*-deficient melanoma cells is enhanced by MICA mAb

We examined whether a MICA/B $\alpha 3$ domain–specific antibody could enhance NK cell–mediated immunity against human *B2M*-deficient tumor cells. We inactivated the *B2M* gene in human A375 melanoma cells, which resulted in a complete loss of MHC-I surface proteins, even following stimulation with IFN γ (Fig. 1A, Supplementary Fig. S1A–B). *B2M*

deficiency did not abolish MICA/B expression, although we noted a ~50% decrease of cell surface expression. Both *B2M*-KO and control A375 cell lines exhibited similar shedding of MICA into the supernatant (Fig. 1B). Treatment with a MICA/B α 3 domain-specific mAb (7C6-hIgG1) inhibited MICA shedding and increased surface expression of MICA/B proteins for both control and *B2M*-deficient A375 cells (Fig. 1B–D).

NK cells express inhibitory receptors for MHC-I molecules (12), and we hypothesized that *B2M*-deficient tumor cells may be more sensitive to MICA/B mAb treatment. We studied the kinetics of NK cell-mediated killing of A375 cells using an imaging-based system that enabled counting of fluorescent tumor cells in 96-well plates at multiple timepoints (33). NK-cell MICA/B mAb treatment (7C6-hIgG1) was more effective against *B2M*-KO compared to control A375 melanoma cells. Even at a low effector-to-target ratio (1:1), only a small number of fluorescent *B2M*-KO melanoma cells remained at late timepoints (48–72 hours) in the presence of the MICA/B mAb (Fig. 1E). We previously established that the 7C6 mAb induces dual engagement of NKG2D and CD16a receptors in human NK cells and that both receptors contribute to NK cell-mediated killing of target cells (23). KIR2DL2, KIR2DL3, and KIR2DL4 are well-characterized inhibitory receptors for MHC-I molecules on human NK cells (12). Although NK cells from healthy donors are likely alloreactive to A375 cells due to MHC mismatch, antibody-mediated blockade of those receptors increased NK cell-mediated killing of 7C6-hIgG1-treated A375 cells (Supplementary Fig. S1C), which suggested that at least some of the NK-cell inhibitory receptors recognized MHC-I proteins on A375 cells. Altogether, these experiments demonstrated that loss of MHC class I surface expression rendered human tumor cells more vulnerable to NK cells, which was further enhanced by a MICA/B mAb.

MICA/B antibody induces immunity against metastases resistant to cytotoxic T cells

We used two murine models to investigate whether MICA/B mAb treatment could induce immunity against tumors with inactivating mutations in the MHC-I and IFN γ pathways (*B2m* and *Jak1* mutations, respectively). IFN γ is secreted by both T cells and NK cells, and IFN γ signaling in tumor cells enhances expression of many genes of the MHC class I pathway and inhibits tumor cell proliferation (3). Therefore, *Jak1* mutations could either negatively impact the ability of NK cells to control tumor cell growth or enhance NK-cell activation through loss of MHC class I proteins that engage inhibitory receptors on NK cells. B16F10 melanoma and LLC1 lung cancer cell lines were transduced to express human MICA, which binds to the murine NKG2D receptor (23). These murine models had differences in their pattern of MHC class I expression. B16F10 melanoma cells had low basal surface expression of H-2K^b and H-2D^b proteins, but exposure to IFN γ increased H-2K^b and H-2D^b surface proteins (Fig. 2A, Supplementary Fig. S2A–B). We inactivated *B2m* or *Jak1* genes in B16F10-MICA cells, which caused resistance to CD8⁺ T cell-mediated killing (Fig. 2A, Supplementary Figures S2–S3), and tested the efficacy of MICA/B mAb treatment in a lung metastasis model. Edited tumor cells were injected intravenously, and treatment was initiated on day 7 when established surface lung metastases were detected (Fig. 2B). B cell-deficient *Ighm*^{-/-} mice were used as hosts to prevent development of endogenous antibodies against human MICA, as previously reported (23). Treatment with the MICA/B mAb (7C6-mIgG2a) inhibited the outgrowth of lung metastases

by control, *B2m*-KO, and *Jak1*-KO B16F10-MICA cells (Fig. 2B). MICA/B mAb treatment also reduced MICA shedding detected in plasma (Supplementary Fig. S5A). We also analyzed the survival of wild-type (*Ighm*^{+/+}) mice inoculated with B16F10-MICA cell lines and treated with MICA/B or control mAbs. Antibodies were administered on days 1 and 2 relative to B16F10-MICA inoculation, which was earlier than the generation of endogenous MICA antibodies by the murine immune system. 7C6 compared to isotype treatment increased survival of WT mice with control, *B2m*-KO, or *Jak1*-KO melanoma metastases (Fig. 2C).

We also examined the efficacy of MICA/B antibody treatment in the LLC1-MICA tumor model. LLC1 lung tumor cells had basal H-2K^b, but not H-2D^b, expression. The surface H-2K^b expression was increased by IFN γ treatment (Fig. 3A). We knocked out the *B2m* gene in this cell line (Supplementary Figure S4B). Control LLC1 cells expressed H-2K^b at baseline and treatment with IFN γ increased MHC-I surface protein expression, whereas *B2m*-KO LLC1 cells had no MHC-I expression, even following IFN γ treatment (Fig. 3A). Tumor cells were injected intravenously into WT mice, and mAb treatment was initiated on day 2. MICA/B mAb treatment reduced the number of lung metastases formed by control LLC1-MICA tumor cells. Inactivation of the *B2m* gene reduced the number of lung metastases compared to control LLC1-MICA cells to almost undetectable levels. We therefore increased the number of inoculated tumor cells by 50%, which resulted in formation of lung metastases by *B2m*-KO LLC1-MICA cells. We observed a reduction in the number of *B2m*-KO LLC1-MICA metastases following treatment with 7C6-mIgG2a compared to the isotype (Fig. 3B).

NK-cell inhibitory receptors for MHC-I are encoded by polymorphic genes and have specificity for polymorphic variants of MHC-I proteins (35). C57BL/6 mice and Balb/c mice differ in their MHC-I polymorphic variants, and as consequence, the F1 generation from the cross between these two mouse strains (called CB6F1) has a population of NK cells that is not tolerant to the MHC-I variants from the C57BL/6 strain (36). Such alloreactive NK cells are key to the therapeutic efficacy of allogeneic stem cell transplantation for leukemia (37). The LLC1 cell line is syngeneic to C57BL/6 mice. *Rag2*^{-/-}*Il2rg*^{-/-} KO mice were reconstituted with either syngeneic NK cells (from C57BL/6 mice) or allogeneic NK cells (from CB6F1 mice). Both syngeneic and allogeneic NK cells significantly reduced the number of lung metastases formed by LLC1-MICA tumor cells when mice were treated with MICA/B versus isotype control mAb. Also, MICA/B antibody treatment was more effective when allogeneic NK cells were transferred (Fig. 3C). Altogether, the data were consistent with the hypothesis that engagement of MHC-I proteins by inhibitory receptors on NK cells reduces the antitumor immunity induced by the MICA/B mAb.

Essential role of NK cells for efficacy of the MICA/B antibody

We next performed mechanistic experiments with the B16F10-MICA cell line inoculated into WT mice. Depletion of NK cells, but not of CD8⁺ T cells, resulted in a complete loss of MICA/B mAb efficacy against both control and *B2m*-KO B16F10-MICA cells, whereas NK-cell depletion reduced MICA/B mAb efficacy against *Jak1*-KO B16F10-MICA cells (Fig. 4A). We also examined lung-infiltrating NK cells by flow cytometry, which were

distinguished from blood NK cells by intravenous injection of anti-CD45.2 prior to euthanasia, as reported previously (23). MICA/B mAb treatment increased the degree of NK-cell infiltration into control or *Jak1*-KO B16F10-MICA tumors (Fig. 4B). In this analysis, NK-cell infiltration was normalized to tumor burden because the number of B16F10-MICA cells was substantially reduced in MICA/B mAb-treated mice (Fig. 4C–D). We did not observe significant differences in NKG2D and CD16 expression by tissue-infiltrating NK cells depending on the genotype of B16F10-MICA melanoma cells, except for an increase in CD16 for NK cells in the *Jak1*-KO B16F10-MICA lung metastasis model following treatment with 7C6-mIgG2a (Supplementary Figure S5). These data demonstrated that MICA/B mAb treatment inhibited the outgrowth of melanoma metastases in a NK cell-dependent manner, even when tumor cells carried inactivating mutations in *B2m* or *Jak1* genes.

Combination therapy that enhances MICA/B protein levels on surface of tumors

In the tumor models described above, MICA transcription was controlled by a heterologous promoter (23). However, in human cancers, MICA/B expression is induced in response to DNA damage and cellular stress (13). The transcription of *MICA* and *MICB* genes is epigenetically regulated by HDACs, and HDAC inhibitors enhance transcription of these genes (27,28). The pan-HDAC inhibitor panobinostat has been FDA-approved for the treatment of multiple myeloma (39) and an intact immune system is required for its therapeutic activity in experimental animal models (40). We therefore examined whether the combination of panobinostat and 7C6-hIgG1 could enhance MICA/B protein expression by increasing transcription of *MICA/B* genes (via panobinostat) and stabilization of the encoded protein on the cell surface (via the MICA/B mAb). RNA-seq analysis and qPCR analysis demonstrated that treatment of A375 cells with panobinostat for 24 hours increased mRNA of multiple genes encoding NKG2D ligands (Fig. 5A–B). As expected, panobinostat also affected transcription of many other genes in A375 melanoma cells, some of which represented immune-related pathways (Supplementary Figure S6). Surface MICA/B protein expression was increased by the combination of panobinostat and MICA/B mAb, and the concentration of shed MICA was diminished without a reduction in cellular viability (Fig. 5C–D). We also examined MICA/B protein expression by a panel of short-term human melanoma cell lines established from metastatic lesions (23,31). Treatment with panobinostat plus MICA/B mAb increased the surface density of MICA/B proteins compared to treatment with individual compounds (Fig. 5E, Supplementary Figure S7). These conclusions were further supported by analysis of a diverse panel of human tumor cell lines (Supplementary Fig. S8). However, MICB shedding could not be analyzed because the ELISA was specific for MICA (Supplementary Figure S9). These data demonstrated that combinatorial approaches which increase transcription of *MICA/B* genes and stabilize synthesized proteins increase surface MICA/B proteins on human cancer cells.

Efficacy of MICA/B mAb and panobinostat combination therapy in a humanized mouse model

We next investigated the *in vivo* activity of panobinostat on surface MICA/B protein expression on human melanoma cells. The selected dose of panobinostat (10 mg/kg) was based on previous research that established its efficacy for multiple myeloma in mouse

models (41). We first established that the selected dose of panobinostat did not negatively impact human NK cells transferred to immunodeficient NSG mice (based on number of circulating total NK cells and percentage of CD16a⁺ or NKG2D⁺ NK cells; Supplementary Fig. S10A–C). Next, we injected ZsGreen⁺ A375 melanoma cells intravenously into NSG mice and waited for two weeks until metastases were established. Mice were then treated twice at a 24-hour interval with panobinostat (or PBS), MICA/B mAb (or isotype control mAb), or the combination of panobinostat plus MICA/B mAb (or panobinostat plus isotype control mAb). One day later, MICA/B surface protein was quantified on ZsGreen⁺ tumor cells from dissociated lung tissue by flow cytometry. The selected dose of panobinostat did not significantly increase MICA/B protein on melanoma cells as a monotherapy, but the combination of panobinostat and MICA/B mAb resulted in high MICA/B surface expression on ZsGreen⁺ A375 cells in pulmonary metastases (Fig. 6A, Supplementary Figure S10D).

Based on our prior experience, survival of transferred human NK cells is limited in NSG mice, and only a small number of human NK cells infiltrate lung tissue (23). We therefore initiated treatment one day following inoculation of A375 cells (Fig. 6B). The early start of treatment likely enabled NK-cell recognition of tumor cells that had not yet infiltrated deeply into the lungs. We found that only the combination of panobinostat plus MICA/B mAb reduced the number of lung metastases formed by control (*B2M*-WT) A375 cells, whereas monotherapy with either panobinostat or MICA/B mAb was ineffective. In contrast, monotherapy with the MICA/B mAb reduced the number of lung metastases formed by *B2M*-KO A375 cells (Fig. 6C). The combination of MICA/B mAb and panobinostat did not enhance this effect against *B2M*-KO metastases, potentially because NK-cell reconstitution was limited in this model. These results demonstrated that MICA/B mAb treatment was more effective against MHC-I-deficient melanoma metastases in this humanized mouse model, whereas only the combination therapy was effective against melanoma metastases that expressed MHC-I proteins.

DISCUSSION

Primary and secondary resistance to checkpoint blockade are major issues in oncology. Many mechanisms of resistance to checkpoint blockade are related to the MHC-I and IFN γ signaling pathways in tumor cells. These include mutations of *B2M* or other genes in the MHC-I antigen presentation pathway, epigenetic silencing of neoantigen or MHC-I expression, and inactivating mutations in the IFN γ signaling pathway (4–6). Although MICA/B proteins have a similar overall structure to MHC-I proteins, they do not assemble with β 2-microglobulin (24). Also, transcription of the *MICA/B* genes is induced by DNA damage and cellular stress rather than by IFN γ (13). Therefore, inactivating mutations in the MHC-I and IFN γ pathway do not abrogate MICA/B expression.

It is well known that loss of MHC-I expression removes an important inhibitory signal for NK cells, but sufficient activating signals are required for induction of NK cell-mediated tumor immunity (12). We showed that metastases with inactivating mutations in the MHC-I (*B2M* mutation) or IFN γ signaling (*JAK1* mutation) pathways can be treated with a MICA/B α 3 domain-specific antibody. This antibody inhibited proteolytic shedding of MICA/B, a common evasion mechanism from NKG2D receptor-mediated immunity in

human cancers. We previously showed that treatment with this mAb induces activation of both NKG2D (increased density of MICA/B ligand) and CD16a (Fc region of mAb) receptors on NK cells and that tumor immunity elicited by this mAb is NK cell–dependent (23). The NKG2D receptor is also expressed by human CD8⁺ T cells, $\gamma\delta$ T cells, and ILCs (14,42,43,44). MICA/B mAb treatment therefore also has the potential to enhance T cell–mediated tumor immunity via the NKG2D receptor expressed by CD8⁺ T cells, although this hypothesis will need to be further investigated. Shedding of some NKG2D ligands does not result in immune escape. For example, the shedding of MULT-1, a murine NKG2D ligand, promotes the NK cell–mediated immunity (45). How shedding of NKG2D ligands other than MICA/B potentially affects NKG2D-mediated immunity in the context of MICA/B mAb treatment remains to be investigated.

Many therapeutic approaches used in oncology enhance expression of MICA/B proteins by tumor cells. However, proteolytic shedding of MICA/B proteins by tumor cells limits the effect of such drugs on NKG2D receptor activation. We showed that the combination of panobinostat and a MICA/B α 3 domain antibody increased MICA/B surface protein expression on tumor cells *in vivo* and enhanced NK cell–mediated immunity against melanoma metastases. The HDAC inhibitor may also induce expression of NKG2D ligands in healthy tissues, but this aspect could not be evaluated in our study because mice do not have *MICA/B* genes. We acknowledge that this humanized model has significant limitations, especially with respect to limited survival of transferred human NK cells due to lack of homeostatic cytokine signaling. A similar conceptual approach could be used to develop combination therapies with other FDA-approved drugs. Also, it is known that the DNA damage response induced by radiation therapy enhances MICA/B transcription (46). A combination of local radiotherapy and systemic immunotherapy with a MICA/B mAb could be used to limit immune-related adverse events observed with combinations involving two systemic immunotherapy agents (such as PD-1 and CTLA-4 mAbs). A clinical trial has already shown that radiation therapy in combination with CTLA-4 blockade can induce abscopal effects (47).

In summary, we showed that metastases with mutations that cause resistance to cytotoxic T cells can be targeted by NK cells when MICA/B shedding is inhibited with a mAb. Two conceptual approaches could be envisioned for eliciting NK cell–mediated tumor immunity with such an antibody. First, a MICA/B α 3 domain–specific mAb could be used to treat tumors resistant to checkpoint blockade due to inactivating mutations in the MHC-I or IFN γ signaling pathways. Second, simultaneous administration of an anti-MICA/B and anti-PD-1 could activate both NK cells and CD8⁺ T cells, thereby preventing the outgrowth of tumor clones resistant to cytotoxic T cells. Induction of NK cell–mediated immunity may thus provide a strategy to treat tumors with escape mutations from T cell–mediated cytotoxicity.

Supplementary Material

Refer to Web version on PubMed Central for supplementary material.

ACKNOWLEDGEMENTS

The authors thank Hye-Jung Kim, Sandrine Degryse, and Stephanie Dougan for providing some of the mouse lines, as well as Irene Ghobrial and Mahshid Rahmat for providing multiple myeloma cell lines.

Funding: This work was supported by a grant from NIH (NCI R01 CA238039 to K.W.W.), a Translational Research Grant from the Leukemia & Lymphoma Society (to K.W.W.) and a sponsored research agreement with Bristol-Myers Squibb (BMS). L.F.A. was supported by a Friends for Life Neuroblastoma Fellowship, SK was supported by an AACR-AstraZeneca fellowship, D.P. by a Cancer Research Institute/Robertson Foundation Fellowship and A.M.L. was supported by a Cancer Immunology Training Grant (T32 CA207021).

REFERENCES

- Ribas A, Wolchok JD, Cancer immunotherapy using checkpoint blockade. *Science* 359, 1350–1355 (2018). [PubMed: 29567705]
- Schumacher TN, Schreiber RD, Neoantigens in cancer immunotherapy. *Science* 348, 69–74 (2015). [PubMed: 25838375]
- Parker BS, Rautela J, Hertzog PJ, Antitumour actions of interferons: implications for cancer therapy. *Nat Rev Cancer* 16, 131–144 (2016). [PubMed: 26911188]
- Gao J et al., Loss of IFN- γ pathway genes in tumor cells as a mechanism of resistance to anti-CTLA-4 therapy. *Cell* 167, 397–404 (2016). [PubMed: 27667683]
- Zaretsky JM et al., Mutations Associated with Acquired Resistance to PD-1 Blockade in Melanoma. *N Engl J Med* 375, 819–829 (2016). [PubMed: 27433843]
- Pitt JM et al., Resistance Mechanisms to Immune-Checkpoint Blockade in Cancer: Tumor-Intrinsic and -Extrinsic Factors. *Immunity* 44, 1255–1269 (2016). [PubMed: 27332730]
- Snyder A et al., Genetic basis for clinical response to CTLA-4 blockade in melanoma. *N Engl J Med* 371, 2189–2199 (2014). [PubMed: 25409260]
- Rizvi NA et al., Cancer immunology. Mutational landscape determines sensitivity to PD-1 blockade in non-small cell lung cancer. *Science* 348, 124–128 (2015). [PubMed: 25765070]
- Hellmann MD et al., Nivolumab plus Ipilimumab in Lung Cancer with a High Tumor Mutational Burden. *N Engl J Med* 378, 2093–2104 (2018). [PubMed: 29658845]
- Hellmann MD et al., Tumor Mutational Burden and Efficacy of Nivolumab Monotherapy and in Combination with Ipilimumab in Small-Cell Lung Cancer. *Cancer Cell* 33, 853–861 (2018). [PubMed: 29731394]
- June CH, O'Connor RS, Kawalekar OU, Ghassemi S, Milone MC, CAR T cell immunotherapy for human cancer. *Science* 359, 1361–1365 (2018). [PubMed: 29567707]
- Long EO, Kim HS, Liu D, Peterson ME, Rajagopalan S, Controlling natural killer cell responses: integration of signals for activation and inhibition. *Annu Rev Immunol* 31, 227–258 (2013). [PubMed: 23516982]
- Raulet DH, Gasser S, Gowen BG, Deng W, Jung H, Regulation of ligands for the NKG2D activating receptor. *Annu Rev Immunol* 31, 413–441 (2013). [PubMed: 23298206]
- Bauer S et al., Activation of NK cells and T cells by NKG2D, a receptor for stress-inducible MICA. *Science* 285, 727–729 (1999). [PubMed: 10426993]
- Salih HR, Rammensee HG, Steinle A, Cutting edge: down-regulation of MICA on human tumors by proteolytic shedding. *J Immunol* 169, 4098–4102 (2002). [PubMed: 12370336]
- Kaiser BK et al., Disulphide-isomerase-enabled shedding of tumour-associated NKG2D ligands. *Nature* 447, 482–486 (2007). [PubMed: 17495932]
- Jinushi M et al., MHC class I chain-related protein A antibodies and shedding are associated with the progression of multiple myeloma. *Proc Natl Acad Sci U S A* 105, 1285–1290 (2008). [PubMed: 18202175]
- Yang FQ et al., Matrix metalloproteinase 2 (MMP2) mediates MHC class I polypeptide-related sequence A (MICA) shedding in renal cell carcinoma. *Actas Urol Esp* 38, 172–178 (2014). [PubMed: 24461475]

19. Boutet P et al., Cutting edge: the metalloproteinase ADAM17/TNF-alpha-converting enzyme regulates proteolytic shedding of the MHC class I-related chain B protein. *J Immunol* 182, 49–53 (2009). [PubMed: 19109134]
20. Groh V, Wu J, Yee C, Spies T, Tumour-derived soluble MIC ligands impair expression of NKG2D and T-cell activation. *Nature* 419, 734–738 (2002). [PubMed: 12384702]
21. Waldhauer I et al., Tumor-associated MICA is shed by ADAM proteases. *Cancer Res* 68, 6368–6376 (2008). [PubMed: 18676862]
22. Salih HR, Goehlsdorf D, Steinle A, Release of MICB molecules by tumor cells: mechanism and soluble MICB in sera of cancer patients. *Hum Immunol* 67, 188–195 (2006). [PubMed: 16698441]
23. de Andrade LF et al., Antibody-mediated inhibition of MICA and MICB shedding promotes NK cell-driven tumor immunity. *Science* 359, 1537–1542 (2018). [PubMed: 29599246]
24. Li P et al., Complex structure of the activating immunoreceptor NKG2D and its MHC class I-like ligand MICA. *Nat Immunol* 2, 443–451 (2001). [PubMed: 11323699]
25. Bahram S, Bresnahan M, Geraghty DE, Spies T, A second lineage of mammalian major histocompatibility complex class I genes. *Proc Natl Acad Sci U S A* 91, 6259–6263 (1994). [PubMed: 8022771]
26. Groh V et al., Cell stress-regulated human major histocompatibility complex class I gene expressed in gastrointestinal epithelium. *Proc Natl Acad Sci U S A* 93, 12445–12450 (1996). [PubMed: 8901601]
27. Armeanu S et al., Natural killer cell-mediated lysis of hepatoma cells via specific induction of NKG2D ligands by the histone deacetylase inhibitor sodium valproate. *Cancer Res* 65, 6321–6329 (2005). [PubMed: 16024634]
28. Skov S et al., Cancer cells become susceptible to natural killer cell killing after exposure to histone deacetylase inhibitors due to glycogen synthase kinase-3-dependent expression of MHC class I-related chain A and B. *Cancer Res* 65, 11136–11145 (2005). [PubMed: 16322264]
29. Zhang C, Wang Y, Zhou Z, Zhang J, Tian Z, Sodium butyrate upregulates expression of NKG2D ligand MICA/B in HeLa and HepG2 cell lines and increases their susceptibility to NK lysis. *Cancer Immunol Immunother* 58, 1275–1285 (2009). [PubMed: 19139882]
30. Diermayr S et al., NKG2D ligand expression in AML increases in response to HDAC inhibitor valproic acid and contributes to allorecognition by NK-cell lines with single KIR-HLA class I specificities. *Blood* 111, 1428–1436 (2008). [PubMed: 17993609]
31. Izar B et al., Bidirectional cross talk between patient-derived melanoma and cancer-associated fibroblasts promotes invasion and proliferation. *Pigment Cell & Melanoma Research* 29, 656–668 (2016). [PubMed: 27482935]
32. Pan D et al., A major chromatin regulator determines resistance of tumor cells to T cell-mediated killing. *Science* 359, 770–775 (2018). [PubMed: 29301958]
33. Chan LL, Wucherpennig KW, de Andrade LF, Visualization and quantification of NK cell-mediated cytotoxicity over extended time periods by image cytometry. *J Immunol Methods* 469, 47–51 (2019). [PubMed: 30951701]
34. Ferrari de Andrade L et al., Natural killer cells are essential for the ability of BRAF inhibitors to control BRAFV600E-mutant metastatic melanoma. *Cancer Res* 74, 7298–7308 (2014). [PubMed: 25351955]
35. Kim S et al., Licensing of natural killer cells by host major histocompatibility complex class I molecules. *Nature* 436, 709–713 (2005). [PubMed: 16079848]
36. Yu YY et al., The role of Ly49A and 5E6(Ly49C) molecules in hybrid resistance mediated by murine natural killer cells against normal T cell blasts. *Immunity* 4, 67–76 (1996). [PubMed: 8574853]
37. Ruggeri L et al., Effectiveness of donor natural killer cell alloreactivity in mismatched hematopoietic transplants. *Science* 295, 2097–2100 (2002). [PubMed: 11896281]
38. Wang X et al., A herpesvirus encoded Qa-1 mimic inhibits natural killer cell cytotoxicity through CD94/NKG2A receptor engagement. *Elife* 7, e38667 (2018). [PubMed: 30575523]
39. Laubach JP, Moreau P, San-Miguel JF, Richardson PG, Panobinostat for the Treatment of Multiple Myeloma. *Clin Cancer Res* 21, 4767–4773 (2015). [PubMed: 26362997]

40. West AC et al., An Intact Immune System Is Required for the Anticancer Activities of Histone Deacetylase Inhibitors. *Cancer Res* 73, 7265–7276 (2013). [PubMed: 24158093]
41. Gowney JD et al. *Blood* 110, 1510–1510 (2007).
42. Groh V, Steinle A, Bauer S, Spies T, Recognition of stress-induced MHC molecules by intestinal epithelial gammadelta T cells. *Science* 279, 1737–1740 (1998). [PubMed: 9497295]
43. Chiossone L, Dumas P-Y, Vienne M, Vivier E, Natural killer cells and other innate lymphoid cells in cancer. *Nature reviews Immunology* 18, 671–688 (2018).
44. Klose CSN et al., Differentiation of type 1 ILCs from a common progenitor to all helper-like innate lymphoid cell lineages. *Cell* 157, 340–356 (2014). [PubMed: 24725403]
45. Deng W et al., A shed NKG2D ligand that promotes natural killer cell activation and tumor rejection. *Science* 348, 136–139 (2015). [PubMed: 25745066]
46. Dhar P, Wu JD, NKG2D and its ligands in cancer. *Curr Opin Immunol* 51, 55–61 (2018). [PubMed: 29525346]
47. Formenti SC et al., Radiotherapy induces responses of lung cancer to CTLA-4 blockade. *Nat Med* 24, 1845–1851 (2018). [PubMed: 30397353]
48. Romee R et al., First-in-human phase 1 clinical study of the IL-15 superagonist complex ALT-803 to treat relapse after transplantation. *Blood* 131, 2515–2527 (2018). [PubMed: 29463563]
49. André P et al., Anti-NKG2A mAb is a checkpoint inhibitor that promotes anti-tumor immunity by unleashing both T and NK cells. *Cell* 175, 1731–1743 (2018). [PubMed: 30503213]

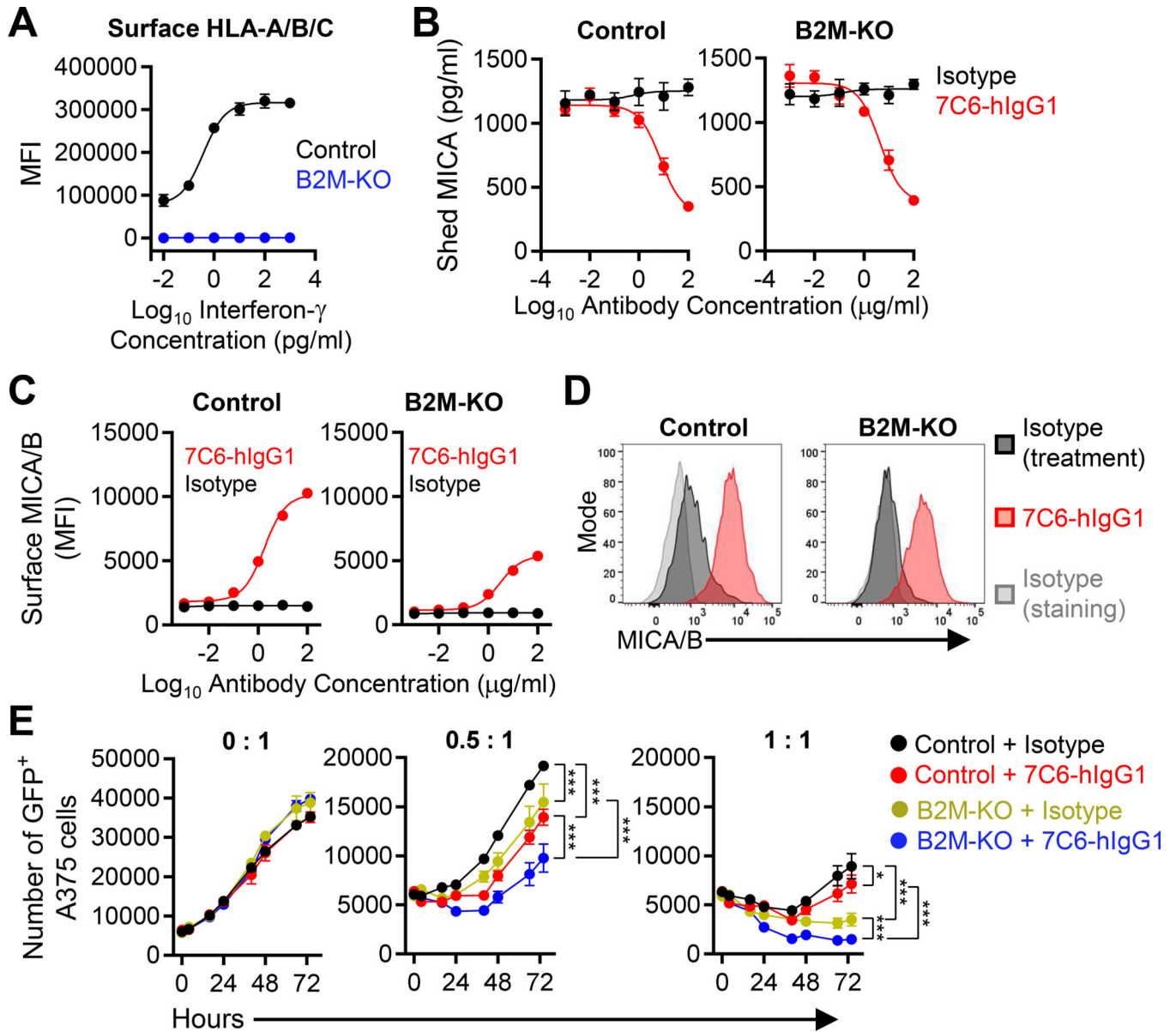


Figure 1. Inactivation of the *B2M* gene enhances NK cell-mediated killing of human melanoma cells in the presence of a MICA/B mAb.

(A) Validation of efficiency of *B2M* gene inactivation. Control or *B2M*-KO human A375 melanoma cells were treated with IFN γ for 24 hours and surface expression of HLA-A/B/C was quantified by flow cytometry. MFI = Mean Fluorescence Intensity. (B-D) Control or *B2M*-KO A375 cells were cultured for 24 hours with MICA/B (7C6-hlgG1) or isotype control antibodies at the indicated concentrations. (B) Quantification of shed MICA released by melanoma cells by sandwich ELISA. (C) MICA/B surface protein on control and *B2M*-KO melanoma cells was quantified by flow cytometry using PE-conjugated MICA/B mAb 6D4 or an isotype control mAb. (D) Histograms representative of the experiment shown in (C). (E) Effect of human NK cells on A375 cells dependent on MHC-I expression and MICA/B mAb treatment. GFP⁺ A375 cells (control or *B2M*-KO) were plated at a density of

5×10^3 cells per well in a 96-well plate and pre-treated with 7C6-hIgG1 or isotype control mAbs (20 $\mu\text{g}/\text{mL}$) for 24 hours prior to addition of purified human NK cells at different effector to target ratios (0:1, 0.5:1 or 1:1). IL-2 (300 U/mL) was added to support NK-cell survival. The number of GFP⁺ A375 cells was quantified by imaging cytometry using a Nexcelom Celigo instrument at multiple timepoints over a 72-hour period. Data representative of three independent experiments (A-E). Statistical analyses were performed by two-way ANOVA with Bonferroni's multiple comparison test (E). Error bars represent standard error (SEM) (A-C and E). * $p < 0.05$, *** $p < 0.001$.

Author Manuscript

Author Manuscript

Author Manuscript

Author Manuscript

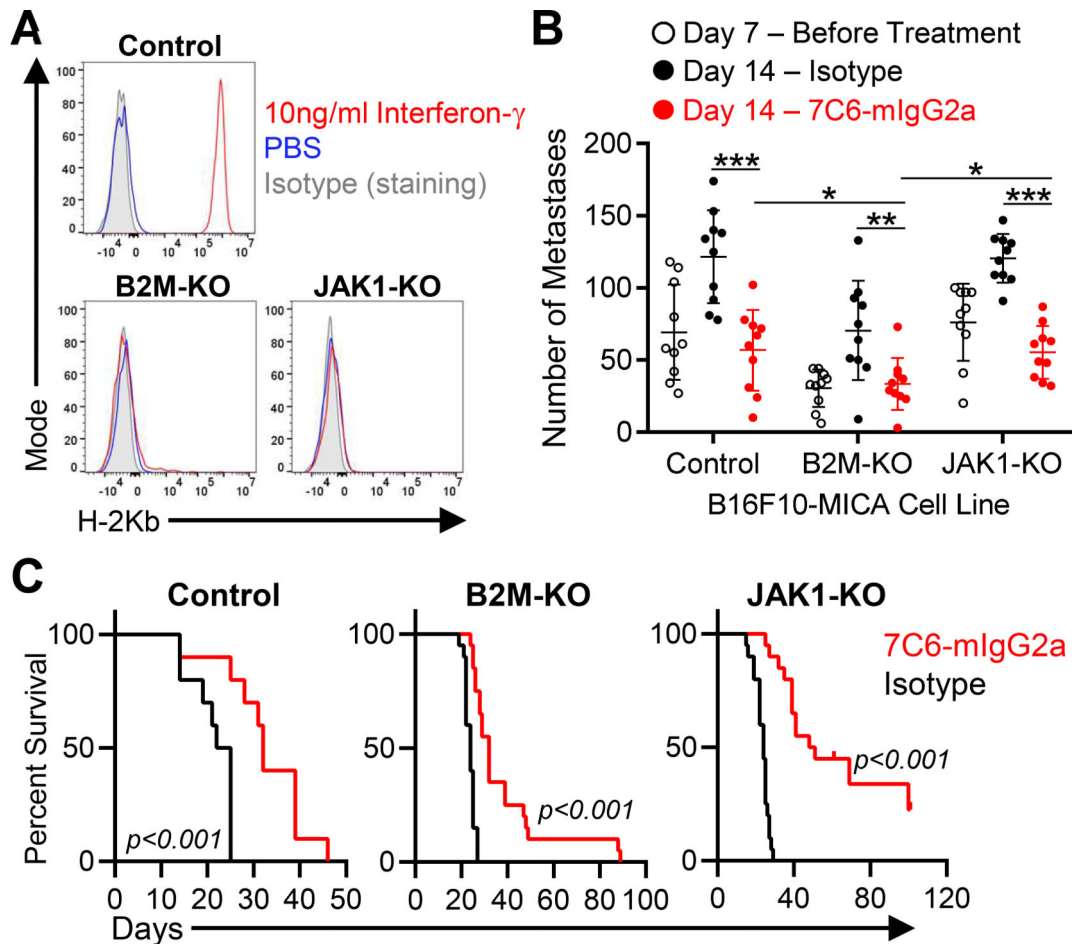


Figure 2. MICA/B mAb treatment induces immunity against melanoma metastases with inactivating mutations in *B2m* and *Jak1* genes.

(A) B16F10-MICA cells (control, *B2m*-KO, or *Jak1*-KO) were treated for 24 hours with IFN γ (10 ng/mL) or solvent control (PBS), and subsequently surface level of H-2K^b was analyzed by flow cytometry. (B) MICA/B mAb treatment effects on established metastases with inactivating mutations in *B2m* or *Jak1* genes. B16F10-MICA cells (7×10^5 control, *B2m*-KO or *Jak1*-KO tumor cells) were injected i.v. into B cell-deficient (*Ighm*^{-/-}) mice. On day 7, a subset of mice was euthanized for quantification of metastases, while the remaining mice were treated with 7C6-mIgG2a or control mAbs (200 μ g i.p. on days 7, 8, and 12). On day 14, lung surface metastases were counted under a stereomicroscope. Each dot represents one mouse and error bars indicate standard deviation (SD). (C) Impact of MICA/B mAb treatment on survival of mice with *B2m* or *Jak1* deficient melanoma metastases. WT mice (*Ighm*^{+/+}) were inoculated i.v. with 2×10^5 control, *B2m*-KO, or *Jak1*-KO B16F10-MICA cells. Mice received 7C6-mIgG2a or isotype control mAbs on days 1 and 2, and mouse survival was recorded. The number of mice per group is as follows: Control (n=10), *B2m*-KO (n=20), and *Jak1*-KO (n=20). Data representative of three independent experiments (A) or pooled from three (B) or two (C) independent experiments. Statistical analyses were performed by two-tailed unpaired Student's t-tests (B), and Log-rank (Mantel-Cox) test (C). * $p < 0.05$, ** $p < 0.01$, *** $p < 0.001$.

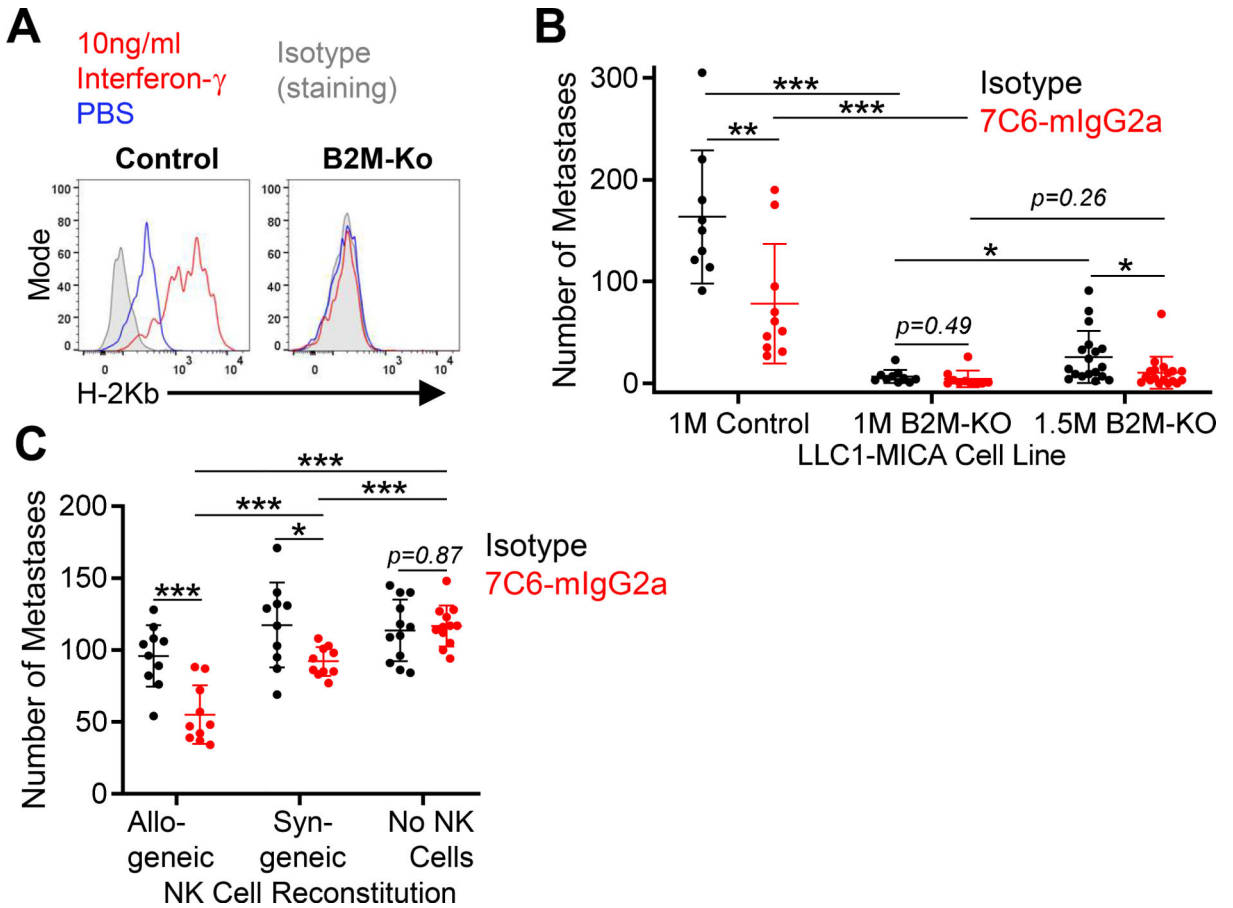


Figure 3. Classical MHC-I molecules expressed by lung cancer cells inhibit NK cells and reduce the efficacy of MICA/B antibody treatment.

(A) Expression of MHC-I by LLC1-MICA cells. Control or *B2m*-KO LLC1-MICA cells were either stimulated with IFN γ (10 ng/mL) or solvent control (PBS) for 24 hours. Surface H-2K^b protein was quantified by flow cytometry. (B) MICA/B mAb treatment of lung metastases formed by LLC1 lung cancer cells. WT C57BL6/J mice were inoculated i.v. with 1×10^6 (1M) or 1.5×10^6 (1.5M) LLC1-MICA tumor cells (control or *B2m*-KO). On day 2 following tumor cell inoculation, mice were treated with indicated mAb (200 μ g i.p.); additional treatments were given on day 3 and then once per week. Lung metastases were counted on day 14. (C) MICA/B mAb treatment of LLC1-MICA metastases in mice reconstituted with allogeneic or syngeneic NK cells. *Rag2*^{-/-}*Il2rg*^{-/-} double-knockout mice were injected with NK cells (2×10^5 cells) from CB6F1/J mice or C56BL/6 mice, which were allogeneic or syngeneic to LLC1 cells, respectively. A third group of *Rag2*^{-/-}*Il2rg*^{-/-} mice did not receive NK cells. LLC1-MICA tumor cells (7×10^5) were injected i.v. 24 hours following NK-cell transfer. On days 2, 3, and then once per week following tumor cell inoculation, mice were treated with the indicated antibodies (200 μ g). Metastases were counted on day 14. Data representative of three independent experiments (A) or pooled from three (B) or two (C) independent experiments. Statistical analyses were performed by two-tailed unpaired Student's t-test (B - C). * $p < 0.05$, ** $p < 0.01$, *** $p < 0.001$. Each dot represents one mouse, and SD is shown (B-C).

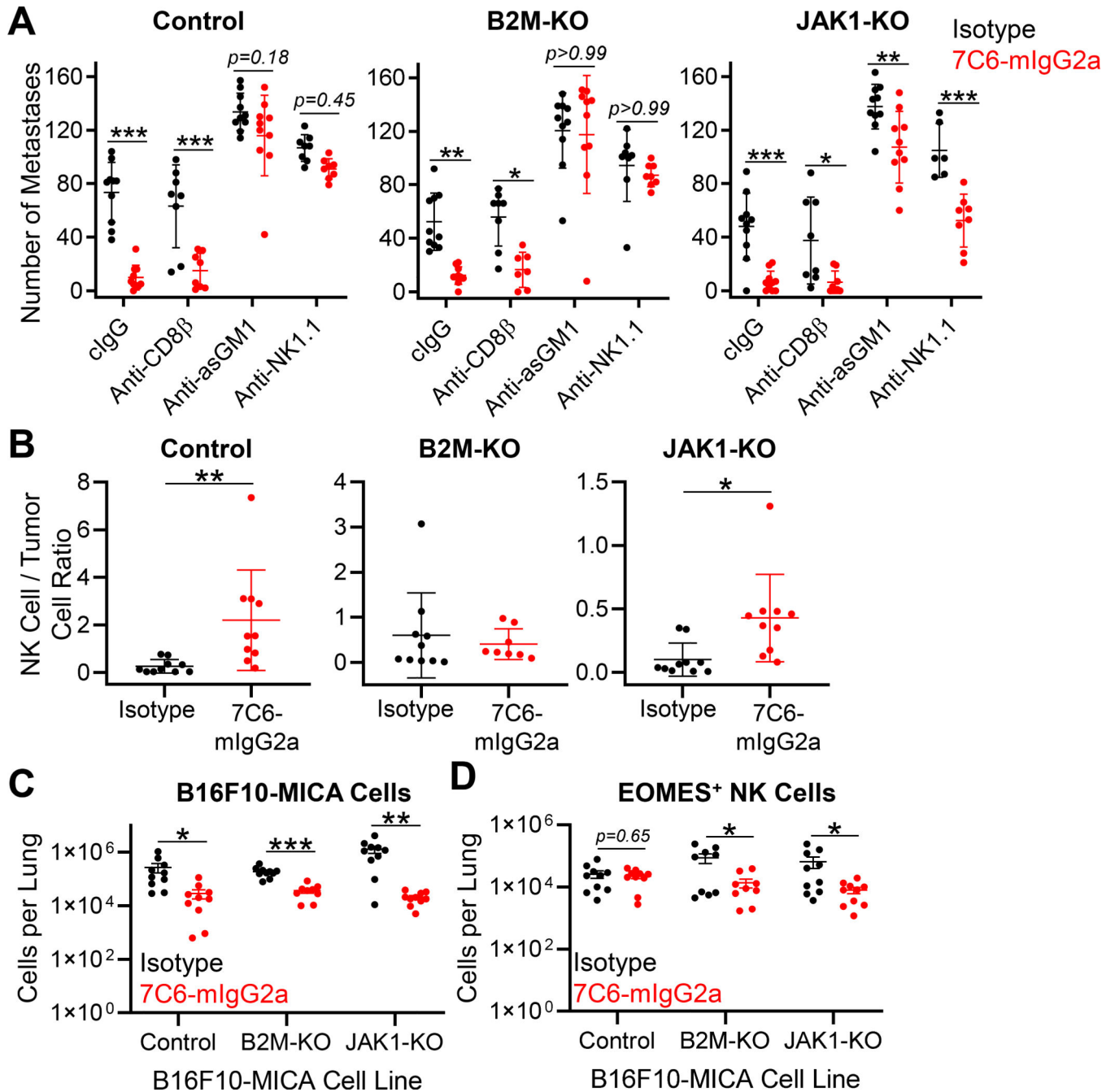


Figure 4. NK cells are essential for treatment of *B2m*- and *Jak1*-deficient melanoma metastases with a MICA/B antibody.

(A) Wild-type (WT) C57BL/6 mice were inoculated i.v. with 7×10^5 B16F10-MICA cells (control, *B2m*-KO, or *Jak1*-KO). Mice were treated with 7C6-mIgG2a or isotype control mAbs (200 μ g) one day later, as well as on days 2 and 7. CD8⁺ T-cell depletion was performed by injection of anti-CD8 β , whereas NK-cell depletion was performed by injection of 100 μ g of anti-asialo GM1 (anti-asGM1) or anti-NK1.1 on days -1, 0, and 7 after tumor cell inoculation. Control mice received an isotype control antibody. Lung surface metastases were quantified on day 14 following tumor inoculation. (B) Analysis of NK-cell

infiltration into lung tissue. Tumor injection and mAb treatment were done as described in (A), with tumor cells that expressed ZsGreen to enable their identification by flow cytometry. On day 12 following tumor cell inoculation, mice were injected i.v. with APC-conjugated anti-CD45.2 to distinguish blood and tissue-infiltrating NK cells, as reported previously (23). Lung-infiltrating NK cells were identified as CD3 ϵ ⁻TCR β ⁻NK1.1⁺CD49b⁺EOMES⁺ viable cells with low staining for CD45.2-APC (injected i.v.) but high staining for CD45.2-PE-CY7 (added to cell suspension). The ratio of NK cells to ZsGreen⁺ B16F10-MICA cells is shown. (C) Numbers of ZsGreen⁺ B16F10-MICA cells and (D) lung-infiltrating NK cells for the indicated genotypes and treatment groups for the experiment described in (B). EOMES labeling was used to differentiate NK cells from ILC1 cells. Data pooled from two independent experiments (A-D). Statistical analyses were performed using two-way ANOVA with Bonferroni's posthoc test (A) or two-tailed unpaired Student's t-test (B-D), *p<0.05, **p<0.01, ***p<0.001. SD (A-B) and SEM (C-D) are shown.

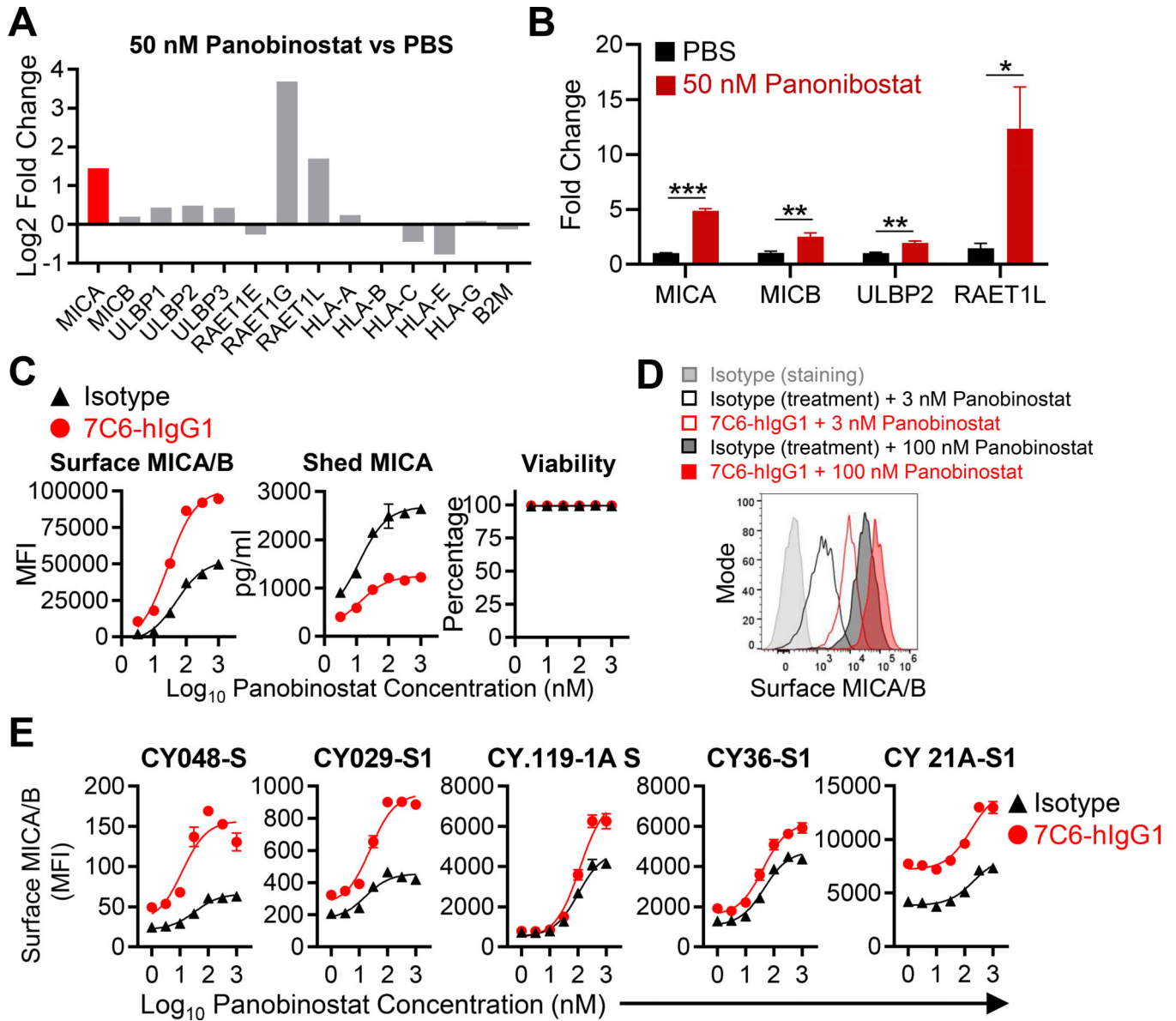


Figure 5. The combination of the HDAC inhibitor panobinostat and a MICA/B mAb enhances surface expression of MICA/B on tumor cells.

(A) NKG2D ligand mRNA expression following treatment with panobinostat. A375 cells were treated for 24 hours with panobinostat (50 nM), and mRNA was extracted for bulk RNA-seq. mRNA expression for NKG2D ligand and MHC class I genes are shown as ratio (log₂ fold-change) for the panobinostat and PBS groups. (B) A375 cells were treated for 24 hours with panobinostat (50 nM) or solvent control (PBS), and the expression of the indicated genes was analyzed by RT-qPCR (triplicates per condition). **p*<0.05, ***p*<0.01, and ****p*<0.001, statistical analysis was performed using two-tailed unpaired Student's *t*-test with Welch's correction. Error bars represent standard deviation of three technical replicates. (C) MICA/B surface protein levels following treatment with panobinostat plus MICA/B mAb. A375 cells were incubated with the indicated mAbs (20 μg/mL) and increasing concentrations of panobinostat for 24 hours. MICA/B surface expression (left)

and A375 cell viability (right) were quantified by flow cytometry. MICA that was shed into the supernatant was quantified by sandwich ELISA (middle). **(D)** Representative histograms of the data shown in (C). **(E)** Treatment of short-term human melanoma cell lines with the combination of panobinostat plus MICA/B mAb. The indicated melanoma cell lines were treated *in vitro* with the indicated mAbs (20 µg/mL) plus increasing concentrations of panobinostat for 24 hours. MICA/B surface expression was quantified by flow cytometry. Cell lines had different basal and induced expression of MICA/B and were ordered from low to high MICA/B expression. Data representative of three independent experiments (B-C and E). SEM are shown (C and E).

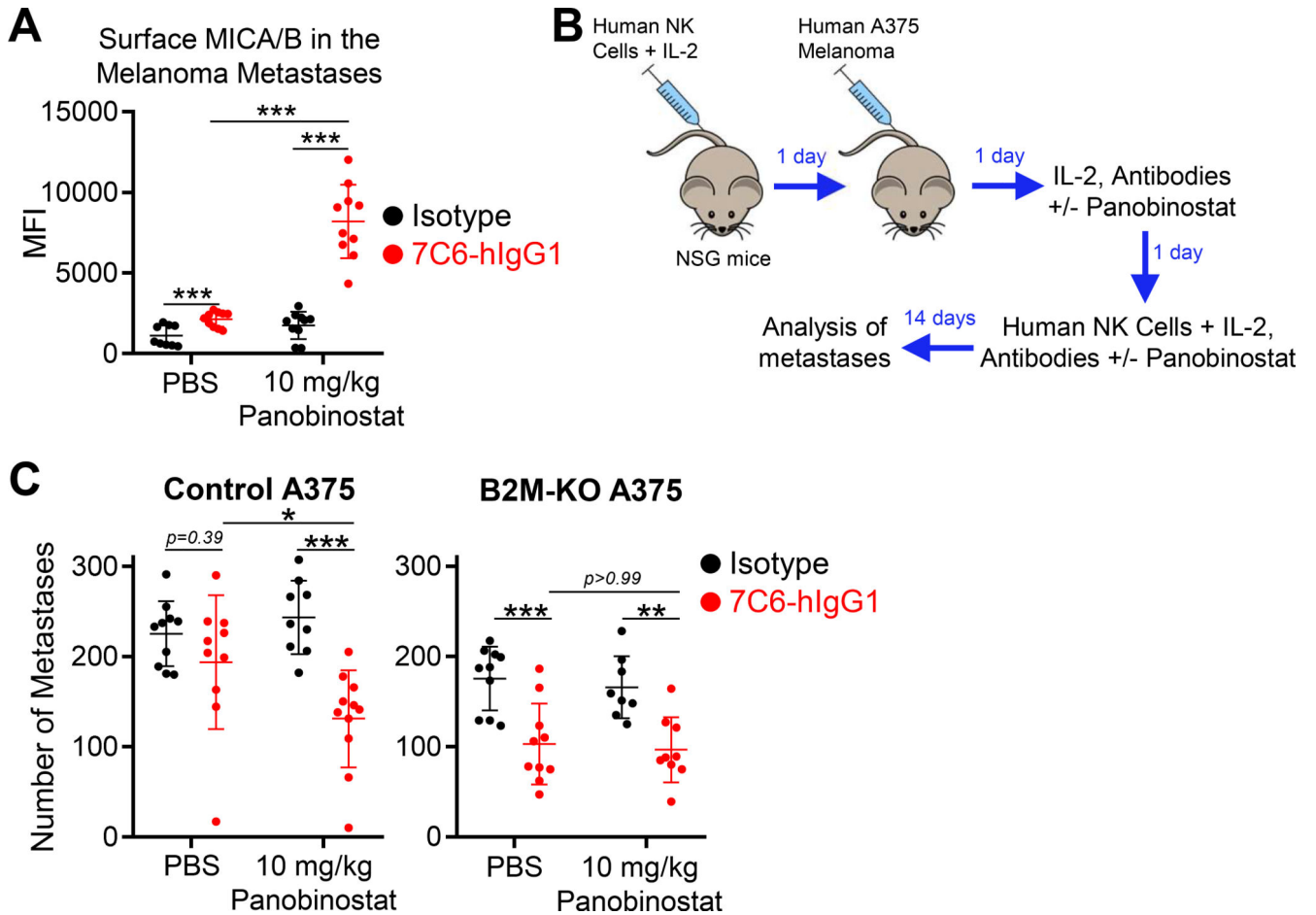


Figure 6. Combination therapy with HDAC inhibitor and MICA/B antibody inhibits growth of metastases in NSG mice reconstituted with human NK cells.

(A) *In vivo* effects of panobinostat plus MICA/B mAb treatment on MICA/B surface protein in metastases formed by human melanoma cells. NSG mice were inoculated i.v. with 1×10^6 ZsGreen⁺ A375 cells. Two weeks later, mice were treated on two subsequent days with the indicated mAbs (200 μ g) +/- panobinostat (10 mg/kg). 24 hours following the last treatment, MICA/B surface expression was analyzed on tumor cells in lung metastases (large, viable, ZsGreen⁺CD45⁻ cells). (B-C) NSG mice were reconstituted with purified human NK cells (2×10^6 i.v.) expanded *in vitro* for 1–3 weeks. *In vivo* survival of NK cells was supported by simultaneous administration of IL2 (7.5×10^4 units) via intraperitoneal injection. On day 1, mice were inoculated i.v. with control or B2M-KO A375 cells (5×10^5). On days 2 and 3, mice received another dose of IL-2, the indicated mAbs (200 μ g) +/- panobinostat (10 mg/kg); on day 3 an additional dose of NK cells was also administered. On day 14, the number of lung surface metastases was counted. (B) Illustration of experimental design and (C) quantification of lung surface metastases. Data pooled from two independent experiments (A and C). Statistical analyses were performed by two-tailed unpaired Student's t-test (A) and two-way ANOVA, Bonferroni's post-hoc test (C), * $p < 0.05$, ** $p < 0.01$, *** $p < 0.001$. Error bars represent SD (A and C).